Int. J. Solids Structures, 1970, Vol. 6, pp. 1211 to 1231. Pergamon Press. Printed in Great Britain

THERMOELASTICITY OF HETEROGENEOUS ORTHOTROPIC CYLINDRICAL SHELLS

Y. STAVSKY and I. SMOLASH

Department of Mechanics, Technion–Israel Institute of Technology, Haifa, Israel

Abstract—The axisymmetric linear quasi-static thermoelastic equations for composite orthotropic cylindrical shells are solved in closed form for fixed-end boundary conditions.

The case of semi-infinite shell is explicitly evaluated and various combinations of laminated shells are examined. It is shown that (1) shell heterogeneity, or the layer reversal effect for two-layer shells, may significantly affect the stress field obtained and its level; (2) the combined action of the composed layers transcends the sum of the individual properties and provides, in many cases, new performance unattainable by the constituents when acting as homogeneous shells; (3) a cross-thermoelastic effect is exhibited by the stress distribution for the considered composite shells.

NOTATION

a	radius of reference surface of shell
$\mathbf{a}, \hat{\mathbf{a}}$	notation of orthotropic layers in relations (60)
A_{ij}	elastic area defined in equation (9)
A_{ij}^*	modified extensional rigidity
b	constant defined in equation (48)
$\mathbf{b}, \hat{\mathbf{b}}$	notation of orthotropic layers in relations (60)
B_1, B_2	constants in equation (40.1)
B_{ij}	elastic statical moment defined in equation (9)
B_{ij}^*	extensional–flexural coupled rigidity
c	constant defined in equation (44.1)
$\mathbf{c}$	notation of isotropic layer in relations (61)
C_1, C_2	constants in equation (40.2)
d	constant defined in equation (44.2)
$\mathbf{d}$	notation of isotropic layer in relations (61)
D_{ij}	elastic moment of inertia defined in equation (9)
D_{ij}^*	modified flexural rigidity
e	subscript denoting *external* layer
$\mathbf{e}$	notation of isotropic layer in relations (61)
E	Young's modulus
E_{ij}	elastic stiffness modulus
f	function defined in equation (29)
F_β, F_ψ	constants defined by expressions (36), (37) respectively
g	decay factor in equation (25)
h	$= h_1 + h_2$, shell thickness, sum of distances to bounding surfaces
i	subscript, subscript denoting *internal* layer in expression for thermal field
j	subscript
k	composite shell parameter defined in equation (20)
K_j	thermal conductivity in $\mathbf{j}$ direction
K	parameter defined in equation (30)
L	functional operator defined in equations (16), (17)
M_ξ, M_θ	axial and circumferential bending moments, respectively
$M_{\xi T}, M_{\theta T}$	thermal quantities defined in equation (10)
N_ξ, N_θ	axial and circumferential forces, respectively
$N_{\xi T}, N_{\theta T}$	thermal quantities defined in equation (10)
p	subscript denoting particular solution in equation (40)

Q	transverse shear force
r	radial coordinate
t_1, t_2	thermal quantities defined in equations (18), (19)
T	temperature change from initial stress-free state
T_i	constants in expression (33) for the temperature
u, w	radial and axial displacements, respectively
z	axial coordinate
α_i	thermal expansion in **i** direction
A_i	thermoelastic coefficient defined in equation (2)
β	slope angle of shell generator
γ_1, γ_2	parameters defined in equations (43)
ε	strain
ζ	thickness coordinate, taken positive inward
θ	circumferential direction
κ	curvature change
ν	Poisson's ratio
ξ	non-dimensional axial coordinate
τ	stress
ϕ_1, ϕ_2	functions defined in equations (41)
Ψ	stress resultant function defined in equation (14.3)

1. INTRODUCTION

THE formulation of the thermoelastic equations of homogeneous media goes back to Duhamel [1, 2] and Neumann [3], about the earlier part of the nineteenth century. Since then substantial efforts have been put in developing the field of thermoelasticity, the results of which are summarized in numerous papers and books, see e.g. the texts by Melan and Parkus [4], Parkus [5], Boley and Weiner [6] and Nowacki [7].

A thermoelastic theory for homogeneous shells of revolution was established by Parkus [8] when the thermal field is axisymmetric and independent of the stress field.

A general quasi-static thermoelastic theory for heterogeneous shells of revolution undergoing symmetrical deformations was recently given by Stavsky [9], assuming that their elastic and thermal properties are rotationally orthotropic.

In what follows Stavsky's [9] equations are specialized for the case of cylindrical shells, solutions for certain thermoelastic problems are obtained and several examples of interest are shown.

2. FORMULATION OF THERMOELASTIC PROBLEM

Consider a thin circular cylindrical shell of constant thickness **h** that is heterogeneous in its thickness direction ζ. The reference cylindrical surface, defined by the radius **a**, is not necessarily taken to be located at mid thickness of shell. A similar assumption was made in the analysis of plates of variable thickness [10] and of heterogeneous shallow shells [11]. The non-dimensional axial coordinate is denoted by $\xi = z/a$ whereas θ designates the circumferential direction (see Fig. 1).

Thermoelastic stress–strain relations

The shell material is assumed to be rotationally orthotropic and so the following Duhamel–Neumann law holds

$$\begin{bmatrix} \tau_\xi \\ \tau_\theta \end{bmatrix} = \begin{bmatrix} E_{\xi\xi} & E_{\xi\theta} & A_\xi \\ E_{\xi\theta} & E_{\theta\theta} & A_\theta \end{bmatrix} \begin{bmatrix} \varepsilon_\xi \\ \varepsilon_\theta \\ T \end{bmatrix} \tag{1}$$

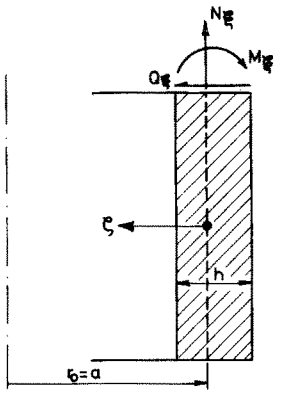

FIG. 1. Cylindrical shell convention.

where the thermal coefficients A_i are given in terms of the elastic stiffnesses E_{ij} and the coefficients of thermal expansion α_i by the relations:

$$-\begin{bmatrix} A_\xi \\ A_\theta \end{bmatrix} = \begin{bmatrix} E_{\xi\xi} & E_{\xi\theta} \\ E_{\xi\theta} & E_{\theta\theta} \end{bmatrix} \begin{bmatrix} \alpha_\xi \\ \alpha_\theta \end{bmatrix}. \tag{2}$$

It is noted that in view of shell heterogeneity

$$E_{ij} = E_{ij}(\zeta), \qquad A_i = A_i(\tau) \qquad (i,j = \xi, \theta) \tag{3}$$

and that T, the change in temperature from the intitial stress-free state, is a given function of ξ and ζ.

The thermal field throughout the shell, which is assumed to be uncoupled with the stress field, is determined by the heat conduction law of Fourier for anisotropic media as given, e.g. in Eringen's [12] monograph. Furthermore, the analysis is restricted to the case where the thermoelastic field is axisymmetric and so the shear stress $\tau_{\xi\theta}$ vanishes identically.

Shell stress–strain relations

Defining reference surface strains, at $\zeta = 0$, and curvature changes as in Stavsky's [9] paper on axisymmetric deformations of heterogeneous shells of revolution, we write:

$$\varepsilon_\xi = \varepsilon_{\xi 0} + \zeta\kappa_\xi \qquad \varepsilon_\theta = \varepsilon_{\theta 0} + \zeta\kappa_\theta \tag{4}$$

where for a small deflections theory of cylindrical shells

$$\varepsilon_{\xi 0} = w'/a, \qquad \varepsilon_{\theta 0} = u/a \tag{5}$$

$$\kappa_\xi = \beta'/a, \qquad \kappa_\theta = 0. \tag{6}$$

The radial and axial displacement components are designated, respectively, by $\mathbf{u}$ and $\mathbf{w}$, whereas β denotes the slope of the shell generator due to deformation. Primes indicate differentiation with respect to the non-dimensional axial coordinate ξ.

Stress resultants and moments are defined by the following integrals over the shell thickness

$$(N_\xi, N_\theta) = \int_{-h_1}^{+h_2} (\tau_\xi, \tau_\theta)\, \mathrm{d}\zeta; \qquad (M_\xi, M_\theta) = \int_{-h_1}^{+h_2} (\tau_\xi, \tau_\theta)\zeta\, \mathrm{d}\zeta \tag{7}$$

which are written, in view of equations (1), in the form:

$$\begin{bmatrix} N_\xi - N_{\xi T} \\ N_\theta - N_{\theta T} \\ M_\xi - M_{\xi T} \\ M_\theta - M_{\theta T} \end{bmatrix} = \left[\begin{array}{cc|cc} A_{\xi\xi} & A_{\xi\theta} & B_{\xi\xi} & B_{\xi\theta} \\ A_{\xi\theta} & A_{\theta\theta} & B_{\xi\theta} & B_{\theta\theta} \\ \hline B_{\xi\xi} & B_{\xi\theta} & D_{\xi\xi} & D_{\xi\theta} \\ B_{\xi\theta} & B_{\theta\theta} & D_{\xi\theta} & D_{\theta\theta} \end{array}\right] \begin{bmatrix} \varepsilon_{\xi 0} \\ \varepsilon_{\theta 0} \\ \kappa_\xi \\ \kappa_\theta \end{bmatrix}. \tag{8}$$

The elastic coefficients A_{ij}, B_{ij}, D_{ij} and the thermoelastic quantities N_{iT}, M_{iT} are defined by the following integrals:

$$(A_{ij}, B_{ij}, D_{ij}) = \int_{-h_1}^{+h_2} (1, \zeta, \zeta^2) E_{ij}\, \mathrm{d}\zeta \qquad (i, j = \xi, \theta) \tag{9}$$

$$(N_{iT}, M_{iT}) = \int_{-h_1}^{+h_2} (1, \zeta) A_i T\, \mathrm{d}\zeta \qquad (i = \xi, \theta). \tag{10}$$

The bounding surfaces of the shell are denoted by h_1 and h_2, and the sign convention for stress resultants and couples is shown in Fig. 1.

Small deflections theory

The equations for small deflections of heterogeneous orthotropic circular shells are obtained by setting in the general equations (8.4) and (8.5) of Ref. [9]

$$r = a, \qquad z = a\xi, \qquad \alpha = a, \qquad \sin\phi = 1, \qquad \cos\phi = 0, \qquad \Phi = \frac{\pi}{2} - \beta \tag{11}$$

which now become, after linearization

$$D^*_{\xi\xi}\beta'' - B^*_{\theta\xi}\Psi'' + a\Psi = -a(B^*_{\xi\xi}N'_{\xi T} + B^*_{\theta\xi}N'_{\theta T} + M'_{\xi T}) \tag{12}$$

$$B^*_{\theta\xi}\beta'' - a\beta + A^*_{\theta\theta}\Psi'' = a(A^*_{\theta\xi}N'_{\xi T} + A^*_{\theta\theta}N'_{\theta T}) \tag{13}$$

for the case that only thermal loads are present. The asterisked elastic coefficients are given in terms of the unasterisked coefficients through equations (7.8) of Ref. [9].

The stress resultants and moments are expressed in terms of the stress function Ψ and the change of slope, β, of shell generator, as follows:

$$aN_\theta = \Psi' \qquad aQ = -\Psi \tag{14}$$

$$\begin{bmatrix} M_\xi - M_{\xi T} \\ M_\theta - M_{\theta T} \end{bmatrix} = \left[\begin{array}{cc|cc} -B^*_{\xi\xi} & -B^*_{\theta\xi} & D^*_{\xi\xi} & D^*_{\xi\theta} \\ -B^*_{\xi\theta} & -B^*_{\theta\theta} & D^*_{\theta\xi} & D^*_{\theta\theta} \end{array}\right] \begin{bmatrix} N_\xi - N_{\xi T} \\ N_\theta - N_{\theta T} \\ \kappa_\xi \\ \kappa_\theta \end{bmatrix}. \tag{15}$$

For the detailed derivation one may wish to consult Section 5 of the chapter by Stavsky and Hoff [13].

Linear theory in terms of two single equations for β and Ψ

The simultaneous thermoelastic equations (12) and (13) for β and Ψ are further transformed to two single uncoupled equations:

$$L\beta = \beta^{IV} - 2B^*_{\theta\xi}\frac{a}{k}\beta'' - \frac{a^2}{k}\beta = \frac{1}{k}(A^*_{\theta\theta}at_1'' + B^*_{\theta\xi}at_2'' - a^2t_2) \tag{16}$$

$$L\Psi = \Psi^{IV} - 2B^*_{\theta\xi}\frac{a}{k}\Psi'' + \frac{a^2}{k}\Psi = \frac{1}{k}(-B^*_{\theta\xi}at_1'' + a^2t_1 + D^*_{\xi\xi}at_2'') \tag{17}$$

where the thermal quantities $\mathbf{t}_1$ and $\mathbf{t}_2$ are given in terms of $N_{\xi T}$, $N_{\theta T}$ and $M_{\xi T}$ by the following expressions:

$$t_1 = -B^*_{\xi\xi}N'_{\xi T} - B^*_{\theta\xi}N'_{\theta T} - M'_{\xi T} \tag{18}$$

$$t_2 = A^*_{\theta\xi}N'_{\xi T} + A^*_{\theta\theta}N'_{\theta T}. \tag{19}$$

The coupled extensional-bending parameter $\mathbf{k}$ is defined by:

$$k = A^*_{\theta\theta}D^*_{\xi\xi} + B^{*2}_{\theta\xi} \tag{20}$$

and is independent of the location of the reference surface. This property of $\mathbf{k}$ becomes obvious in view of the invariance properties of the A^*, B^* and D^* matrices as established by Stavsky and Friedland [14].

Boundary conditions

The conditions at a boundary $\xi = \xi_b$ are generally three:

$$u = \bar{u} \quad \text{or} \quad Q = \bar{Q} \tag{21}$$

$$\beta = \bar{\beta} \quad \text{or} \quad M_\xi = \bar{M}_\xi \tag{22}$$

$$w = \bar{w} \quad \text{or} \quad N_\xi = \bar{N}_\xi. \tag{23}$$

In the case of a semi-infinite shell it would be required that the stresses and displacements are bounded as $\xi \to \infty$.

3. SOLUTION FOR SEMI-INFINITE SHELLS

Thermal field

Consider a semi-infinite composite orthotropic cylindrical shell subject to the following steady state thermal boundary conditions

$$T_e = T_e^0 \quad \text{at} \quad \zeta = -h_1 \quad \text{for any} \quad \xi \tag{24}$$

$$T_i = T_e^0 - (T_e^0 - T_i^0)\,e^{-g\xi} \quad \text{at} \quad \zeta = +h_2 \quad \text{for any} \quad \xi \tag{25}$$

where the shell external and internal temperatures at $\xi = 0$ are denoted by T_e^0, T_i^0, respectively, and $\mathbf{g}$ is a given decay factor. (See Fig. 2).

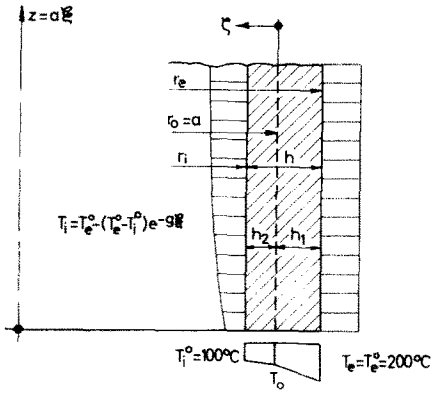

FIG. 2. Semi-infinite two-layer cylindrical shell with temperature distribution.

The thermal field is obtained by solving the steady state heat conduction equation for a solid with cylindrical orthotropy, as given in Carslaw and Jaeger's [15] text

$$\frac{1}{r}K_r(rT_{,r})_{,r}+\frac{1}{r^2}K_\theta T_{,\theta\theta}+K_z T_{,zz}=0 \tag{26}$$

where K_r, K_θ, K_z are the thermal conductivities in the radial, circumferential and axial directions, respectively, of the cylindrical shell.

In view of the axisymmetric boundary conditions (24) and (25) the thermal field is independent of the circumferential coordinate θ and so $T = T(r, z)$. If furthermore K_z is negligibly small as compared to K_r then equation (26) simplifies as follows:

$$\frac{1}{r}K_r(rT_{,r})_{,r}=0. \tag{27}$$

The thermal field so obtained is given by

$$T = T_0+(T_e^0-T_i^0)\,e^{-g\xi}f(\zeta) \tag{28}$$

where the temperature at the reference $\zeta = 0$ is denoted by T_0 and the variation of T across the shell thickness is specified by the function

$$f(\zeta)=\frac{1}{K}K_{rj}\ln(1-\zeta/a) \qquad \begin{matrix} j=e \quad \text{for} \quad 0<\zeta<h_2 \\ j=i \quad \text{for} \quad -h_1<\zeta<0 \end{matrix} \tag{29}$$

for a two-layer cylindrical shell.

The coefficient K is of the form

$$K = K_{re}\ln(a/r_i)+K_{ri}\ln(r_e/a) \tag{30}$$

where K_{re} and K_{ri} are the thermal conductivities in the thickness direction for the external and internal layers, respectively. The internal and external radii of the composite shell are expressed in terms of radius of the reference surface and the layers' dimensions:

$$r_i = a-h_2, \qquad r_e = a+h_1 \tag{31}$$

T_0 is given by the following expression:

$$T_0 = T_e^0 - (T_e^0 - T_i^0)\,\mathrm{e}^{-g\xi}\frac{1}{K}K_{ri}\ln(r_e/a). \tag{32}$$

The temperature distribution, given by equations (28), (32), is conveniently expressed in terms of the constants T_1, T_2 and T_3:

$$T = T_1 + T_2\,\mathrm{e}^{-g\xi} + T_3 f(\zeta)\,\mathrm{e}^{-g\xi} \tag{33}$$

where

$$T_1 = T_e^0, \qquad T_2 = (T_i^0 - T_e^0)\frac{1}{K}K_{ri}\ln(r_e/a), \qquad T_3 = T_e^0 - T_i^0. \tag{34}$$

Solution of differential equations

For the thermal field as specified by expression (33) the shell thermoelastic equations (16) and (17) are written in the following form:

$$L\beta = F_\beta\,\mathrm{e}^{-g\xi}, \qquad L\Psi = F_\Psi\,\mathrm{e}^{-g\xi} \tag{35}$$

where

$$F_\beta = \frac{a^2}{k}g^3\left[\frac{1}{a}A^*_{\theta\theta}(B^*_{\xi\xi}N^{(2)}_{\xi T} + B^*_{\theta\xi}N^{(2)}_{\theta T} + M^{(2)}_{\xi T}) + \left(-\frac{1}{a}B^*_{\theta\xi} + \frac{1}{g^2}\right)(A^*_{\theta\xi}N^{(2)}_{\xi T} + A^*_{\theta\theta}N^{(2)}_{\theta T})\right] \tag{36}$$

$$F_\Psi = \frac{a^2}{k}g^3\left[\left(-\frac{1}{a}B^*_{\theta\xi} + \frac{1}{g^2}\right)(B^*_{\xi\xi}N^{(2)}_{\xi T} + B^*_{\theta\xi}N^{(2)}_{\theta T} + M^{(2)}_{\xi T}) - \frac{1}{a}D^*_{\xi\xi}(A^*_{\theta\xi}N^{(2)}_{\xi T} + A^*_{\theta\theta}N^{(2)}_{\theta T})\right] \tag{37}$$

and the thermal quantities $N^{(2)}_{iT}$ and $M^{(2)}_{iT}$ are related to N_{iT} and M_{iT} through the expressions:

$$N_{iT} = N^{(1)}_{iT} + N^{(2)}_{iT}\,\mathrm{e}^{-g\xi}, \qquad M_{iT} = M^{(1)}_{iT} + M^{(2)}_{iT}\,\mathrm{e}^{-g\xi} \qquad (i = \xi, \theta) \tag{38}$$

where

$$(N^{(1)}_{iT}, M^{(1)}_{iT}) = T_1\int_{-h_1}^{+h_2}(1, \zeta)A_i\,\mathrm{d}\zeta,$$

$$(N^{(2)}_{iT}, M^{(2)}_{iT}) = T_2\int_{-h_1}^{+h_2}(1, \zeta)A_i\,\mathrm{d}\zeta + T_3\int_{-h_1}^{+h_2}(1, \zeta)A_i f(\zeta)\,\mathrm{d}\zeta \qquad (i = \xi, \theta). \tag{39}$$

The complete solution of the differential equations (16) and (17), satisfying regularity conditions at $\xi = \infty$, is given by the following formulas for β and Ψ:

$$\beta = B_1\phi_1 + B_2\phi_2 + \beta_p, \qquad \Psi = C_1\phi_1 + C_2\phi_2 + \Psi_p \tag{40}$$

where

$$\phi_1 = \mathrm{e}^{-\gamma_1\xi}\cos\gamma_2\xi, \qquad \phi_2 = e^{-\gamma_1\xi}\sin\gamma_2\xi \tag{41}$$

$$\beta_p = \beta_{p0}\,\mathrm{e}^{-g\xi}, \qquad \Psi_p = \Psi_{p0}\,\mathrm{e}^{-g\xi}. \tag{42}$$

The non-dimensional parameters γ_1 and γ_2 are defined as:

$$2\gamma_1^2 = d - c, \qquad 2\gamma_2^2 = d + c \tag{43}$$

where

$$c = -B^*_{\theta\xi}a/k, \qquad d = a/\sqrt{k}. \tag{44}$$

The values at $\xi = 0$ of the particular solutions for β and Ψ are expressed in the form

$$\beta_{p0} = F_\beta(g^4+2cg^2+d^2)^{-1}, \qquad \Psi_{p0} = F_\Psi(g^4+2cg^2+d^2)^{-1}. \tag{45}$$

Note that due to the coupling of β and Ψ, as clearly exhibited by the two simultaneous equations (12) and (13), the constants B_1, B_2, C_1 and C_2 are interrelated and the two boundary conditions (21) and (22) are sufficient for their unique determination. In view of the linearized version of the system of equations (12) and (13) one finds

$$aD^*_{\xi\xi}\beta = k\Psi'' - aB^*_{\theta\xi}\Psi \tag{46}$$

and consequently

$$B_1 = -bC_2, \qquad B_2 = bC_1 \tag{47}$$

where

$$b = \sqrt{(A^*_{\theta\theta}/D^*_{\xi\xi})}. \tag{48}$$

Boundary conditions

Consider the boundary conditions of type (21) and (22) in the specific form:

$$u = 0, \qquad \beta = 0 \quad \text{at} \quad \xi = 0 \tag{49}$$

which uniquely determine the constants in equations (40). As for the boundary conditions of type (23) it is assumed that

$$N_\xi = 0 \quad \text{at} \quad \xi = 0; \qquad w = 0 \quad \text{at} \quad \xi = \infty \tag{50}$$

which in view of the shell equilibrium equations in the ξ-direction, equation (5.5) of Ref. [9], yields the result

$$N_\xi \equiv 0 \qquad \text{through the cylindrical shell} \tag{51}$$

whereas

$$w = \int a\varepsilon_{\xi 0}\,\mathrm{d}\xi. \tag{52}$$

The axial strain $\varepsilon_{\xi 0}$ is expressed in terms of the functions β and Ψ by using the first of equations (7.6) as given in Ref. [9]:

$$\varepsilon_{\xi 0} = A^*_{\xi\xi}(-N_{\xi T}) + A^*_{\xi\theta}(N_\theta - N_{\theta T}) + B^*_{\xi\xi}\kappa_\xi + B^*_{\xi\theta}\kappa_\theta \tag{53}$$

and the constant of integration in equation (52) is to be determined by the boundary condition (50.2). Note that the vanishing of N_ξ for the considered shell is independent of the boundary conditions (21), (22) whereas $\mathbf{w}$ is readily determined when β and Ψ are known.

The constants in equations (40) are as follows:

$$B_1 = -\beta_{p0} \tag{54}$$

$$C_1 = [A^*_{\theta\xi}(N^{(1)}_{\xi T}+N^{(2)}_{\xi T}) + A^*_{\theta\theta}(N^{(1)}_{\theta T}+N^{(2)}_{\theta T}) - (\beta_{p0}/a)(B^*_{\theta\xi}\gamma_1 + A^*_{\theta\theta}\gamma_2/b) + (g/a)(A^*_{\theta\theta}\Psi_{p0} + B^*_{\theta\xi}\beta_{p0})] \times [(-A^*_{\theta\theta}\gamma_1 + B^*_{\theta\xi}\gamma_2 b)/a]^{-1} \tag{55}$$

$$B_2 = bC_1, \qquad C_2 = \beta_{p0}/b \tag{56}$$

where β_{p0} is given by the first of equations (45) and b is defined by relation (48).

Having the solution for the basic variables β and Ψ the stress resultants and couples as well as the stress distribution are readily obtained through equations (5), (6), (8) and (1).

4. NUMERICAL EXAMPLES

Some insight into the thermoelastic behavior of composite cylindrical shells will be gained by considering the following three special cases of the thermal field given by equation (33):

Case I

$$g = 0, \qquad T = T_i^0 = T_i = T_e^0 = T_e = 200°C \tag{57}$$

Case II

$$g = 0, \qquad T_i^0 = T_i = 100°C, \qquad T_e^0 = T_e = 200°C \tag{58}$$

Case III

$$g = 480, \qquad T_i^0 = 100°C, \qquad T_e^0 = 200°C. \tag{59}$$

Two-layer cylindrical shells were chosen for numerical evaluation, being composed of various combinations of homogeneous sheets with the following thermo-elastic properties:

Type	$E_{\xi\xi}/E_0$	$E_{\theta\theta}/E_0$	$E_{\xi\theta}/E_0$	α_ξ/α_0	α_θ/α_0	K_r/K_0
a	1	0·5	0.3	0.5	1	0·1
â	0·5	1	0·3	1	0·5	0·1
b	5	0·6	0·7	0·25	1·5	0·7
b̂	0·6	5	0·7	1·5	0·25	0·7

(60)

for the *orthotropic* layers **a**, **â**, **b**, **b̂** and

Type	$\frac{E}{1-\nu^2}/E_0$	ν	α/α_0	K/K_0
c	1	0·3	0·5	0·5
d	5	0·14	0·5	0·1
e	0·6	0·5	0·25	0·1

(61)

for the *isotropic* layers **c**, **d**, **e**. The constants with the subscript "0" have the following numerical values:

$$E_0 = 10^6 \text{ kg/cm}^2, \qquad \alpha_0 = 10^{-5}/°C, \qquad K_0 = 1\frac{\text{cal}}{(\text{sec})(\text{cm}^2)(°C/\text{cm})}. \tag{62}$$

Note that the thermo-elastic properties of the orthotropic material **â** is obtained from those of **a** by interchanging the subscripts ξ and θ. The same holds for the materials **b̂** and **b**.

Of the homogeneous orthotropic layers **a**, **â**, **b**, **b̂** 4 homogeneous shells and 12 two-layer shells were evaluated and the results for the highest stresses in the axial and circumferential directions are summarized in Tables 1, 3 and 5. Of the homogeneous isotropic layers **c**, **d**, **e** 3 homogeneous shells and 6 two-layer shells were analyzed and the values of the extremal stresses are given in Tables 2, 4 and 6. For all homogeneous shells, denoted by Nos. 1–4, and 17–19, $\mathbf{h} = 1$ cm whereas for all two-layer shells, Nos. 5–16 and 20–25, $\mathbf{h}_1 = \mathbf{h}_2 = 0.5$ cm. The radius of the reference surface for all shells considered is $r_0 = a = 400$ cm. As shown in Fig. 3, for the *external* layer $-\mathbf{h}_1 < \zeta < 0$ and for the *internal* layer $0 < \zeta < \mathbf{h}_2$. For brevity we designate by "1", "2", "3" and "4" the fibers located at $\zeta = -\mathbf{h}_1, 0; 0, \mathbf{h}_2$, respectively. Note that locations "2" and "3" refer to the external and internal layers, respectively, at both sides of the reference surface $\zeta = 0$, (see Fig. 5).

Using this notation the ζ and z coordinates of the fibers where the stresses occur are given in the parentheses following their numerical values, as indicated in Tables 1–6. For each shell the first line refers to the *external* layer whereas the second line refers to the *internal* layer. Thus, e.g. shell No. 5 in Table 1 is composed of an external layer **a** and internal layer **b** whereas for shell No. 6 the order of these layers is reversed. The largest compressive axial stress in layer **a** of shell No. 5 is $\tau_\xi = -3455\,\text{kg/cm}^2$ occurring at $\zeta = -0{\cdot}5$ cm, $z = 0$; for shell No. 6 this value drops to $\tau_\xi = -930\,\text{kg/cm}^2$ at $\zeta = +0{\cdot}5$ cm, $z = 34$ cm when **a** is now the external layer. The numerical results were obtained by using an Elliott 503 digital computer.

5. DISCUSSION OF RESULTS

The results for the extremal stresses in the considered composite cylindrical shells, as summarized in Tables 1–6, are noted for the following features:

(a) *Layer inversion effect*

The reversal of layer location, or more generally the shell heterogeneity in the thickness direction, have a major effect on the stress field obtained. Consider shells Nos. 9 and 10 in Table 1, the axial compressive stress in layer **b̂** of shell No. 9 is 40 per cent of the corresponding stress in Shell No. 10, whereas for the circumferential direction this value goes up to 58·5 per cent. For the same shells subject to the thermal field II we get from Table 3 that the axial compressive stress in layer **b̂** of shell No. 9 is only 11·2 per cent of the corresponding stress in shell No. 10, whereas for the θ-direction it goes up to 29·5 per cent. Regarding the thermal field III it is seen from Table 5 that the axial compressive stress in layer **â** of shell No. 8 is 31·6 per cent of the corresponding stress in shell No. 7, whereas in the circumferential direction this value goes up to 42·7 per cent. The axial tensile stress in layer **b** of shell No. 8 is 62·6 per cent of the corresponding stress in shell No. 7. (See Fig. 5). As for the shells composed of isotropic layers mention is made to shell No. 23 in Table 6 where in layer **e** the tensile stress is 43·4 per cent of the corresponding stress in shell No. 22.

(b) *Efficiency of lamination*

Some measure to the efficiency of lamination may be achieved by comparing the stresses obtained for a two-layer shell with those developed in the corresponding homogeneous shells. So, e.g. shell No. 9 (Table 3) composed of layers **a**, **b̂** is compared with

TABLE 1. ORTHOTROPIC LAYERS. CASE I

No.	Layers	τ_ξ (kg/cm^2)				τ_θ (kg/cm^2)				T_0 (°C)
	a	461	(**1**, 30)	−2218	(**1**, 0)	90	(**1**, 46)	−1485	(**1**, 0)	
1										200
	a	2218	(**4**, 0)	−461	(**4**, 30)	35	(**3**, 58)	−820	(**3**, 0)	
	â	230	(**1**, 20·9)	−1109	(**1**, 0)	90	(**1**, 34)	−1485	(**1**, 0)	
2										200
	â	1109	(**4**, 0)	−230	(**4**, 20·9)	35	(**3**, 42)	−820	(**3**, 0)	
	b	1711	(**1**, 42)	−8232	(**1**, 0)	157	(**1**, 66)	−2658	(**1**, 0)	
3										200
	b	8232	(**4**, 0)	−1711	(**4**, 42)	65	(**3**, 86)	−1506	(**3**, 0)	
	b̂	285	(**1**, 14·7)	−1372	(**1**, 0)	214	(**1**, 22)	−3692	(**1**, 0)	
4										200
	b̂	1372	(**4**, 0)	−285	(**4**, 14·7)	90	(**3**, 30)	−2092	(**3**, 0)	
	a	265	(**1**, 38)	−3455	(**1**, 0)	260	(**1**, 58)	−1856	(**1**, 0)	
5										200
	b	7788	(**4**, 0)	−3044	(**3**, 0)	—	—	−1932	(**3**, 0)	
	b	4177	(**2**, 0)	−6654	(**1**, 0)	7	(**1**, 50)	−2438	(**1**, 0)	
6										200
	a	2322	(**4**, 0)	−930	(**4**, 34)	236	(**3**, 70)	−807	(**3**, 3·9)	
	â	—	—	−2421	(**1**, 0)	589	(**1**, 50)	−2273	(**1**, 0)	
7										200
	b	7716	(**4**, 0)	−4049	(**3**, 0)	—	—	−2073	(**3**, 0)	
	b	5577	(**2**, 0)	−6188	(**1**, 0)	—	—	−2372	(**1**, 0)	
8										200
	â	894	(**4**, 0)	−831	(**4**, 26)	620	(**3**, 54)	−1027	(**3**, 2·7)	
	a	1026	(**2**, 0)	−1233	(**1**, 0)	—	—	−1190	(**1**, 0)	
9										200
	b̂	781	(**4**, 0)	−907	(**4**, 16·8)	613	(**3**, 34)	−2771	(**3**, 0·6)	
	b̂	—	—	−2269	(**1**, 0)	506	(**1**, 34)	−4738	(**1**, 0)	
10										200
	a	2720	(**4**, 0)	—	—	—	—	−682	(**3**, 0)	
	â	454	(**1**, 15·7)	−908	(**1**, 0)	—	—	−1365	(**1**, 0)	
11										200
	b̂	1020	(**4**, 0)	−479	(**4**, 15·8)	385	(**3**, 30)	−2476	(**3**, 0)	
	b̂	56	(**1**, 16·8)	−1556	(**1**, 0)	375	(**1**, 30)	−3907	(**1**, 0)	
12										200
	â	1444	(**4**, 0)	−34	(**4**, 16·9)	46	(**4**, 0)	−631	(**3**, 0·8)	
	a	715	(**2**, 0)	−1575	(**1**, 0)	—	—	−1292	(**1**, 0)	
13										200
	â	1002	(**4**, 0)	−519	(**4**, 22)	266	(**3**, 46)	−915	(**3**, 1·4)	
	â	32	(**1**, 26)	−1669	(**1**, 0)	272	(**1**, 42)	−1821	(**1**, 0)	
14										200
	a	2241	(**4**, 0)	−141	(**4**, 26)	—	—	−834	(**3**, 0)	
	b	5762	(**2**, 0)	−5272	(**1**, 0)	—	—	−2244	(**1**, 0)	
15										200
	b̂	417	(**4**, 0)	−1441	(**4**, 18·1)	1246	(**3**, 38)	−3209	(**3**, 1·5)	
	b̂	—	—	−3271	(**1**, 0)	1047	(**1**, 42)	−5908	(**1**, 0)	
16										200
	b	8126	(**4**, 0)	−2908	(**3**, 0)	—	—	−1913	(**3**, 0)	

TABLE 2. ISOTROPIC LAYERS. CASE I

No.	Layers	τ_ξ (kg/cm^2)				τ_θ (kg/cm^2)				T_0 (°C)
	c	340	(**1**, 26)	−1652	(**1**, 0)	74	(**1**, 42)	1406	(**1**, 0)	
17										200
	c	1652	(**4**, 0)	−340	(**4**, 26)	39	(**3**, 50)	−910	(**3**, 0)	
	d	1754	(**1**, 26)	−8575	(**1**, 0)	274	(**1**, 46)	−6102	(**1**, 0)	
18										200
	d	8575	(**4**, 0)	−1754	(**4**, 26)	208	(**3**, 50)	−4902	(**3**, 0)	
	e	93	(**1**, 26)	−450	(**1**, 0)	30	(**1**, 38)	−450	(**1**, 0)	
19										200
	e	450	(**4**, 0)	−93	(**4**, 26)	10	(**3**, 50)	−225	(**3**, 0)	
	c	536	(**1**, 22)	−2922	(**1**, 0)	100	(**1**, 34)	−1787	(**1**, 0)	
20										200
	d	7105	(**4**, 0)	−3353	(**3**, 0)	200	(**3**, 42)	−5371	(**3**, 42)	
	d	3619	(**2**, 0)	−6839	(**1**, 0)	297	(**1**, 38)	−5859	(**1**, 0)	
21										200
	c	2655	(**4**, 0)	−623	(**4**, 20·9)	39	(**3**, 46)	−782	(**3**, 3)	
	c			−1358	(**1**, 0)			−1461	(**1**, 0)	
22										200
	e	1129	(**4**, 0)			340	(**4**, 0)	−10	(**3**, 2·2)	
	e	477	(**1**, 26)	−417	(**1**, 0)	360	(**1**, 38)	−433	(**1**, 0)	
23										200
	c	646	(**4**, 0)	−528	(**4**, 26)			−860	(**3**, 0)	
	d	4048	(**2**, 0)	−6787	(**1**, 0)			−5852	(**1**, 0)	
24										200
	e	2020	(**4**, 0)	−43	(**4**, 19·6)	785	(**4**, 0)			
	e	710	(**1**, 22)	−1602	(**1**, 0)	498	(**1**, 26)	−1026	(**1**, 0)	
25										200
	d	6370	(**4**, 0)	−4466	(**3**, 0)			−5527	(**3**, 0)	

shell No. 1 made of material **a** and with shell No. 4 made of material $\hat{\mathbf{b}}$. All three shells have the same geometry and are subject to the same thermal field and boundary conditions.

It is found that the *axial* tensile and compressive stresses in layer **a** of shell No. 9 is 36·3 per cent and 58 per cent, respectively of the corresponding stresses in shell No. 1, whereas for layer $\hat{\mathbf{b}}$ these values are 42·5 per cent and 17·1 per cent of the corresponding stresses in shell No. 4. The *circumferential* tensile and compressive stresses in layer $\hat{\mathbf{b}}$ of shell No. 9 is 57 per cent and 36·7 per cent of the corresponding stresses in shell No. 4. The reduction in the circumferential compressive stress in layer **a** of shell No. 9 is not as high as the previous figures and stands on 81·8 per cent of the corresponding stress in shell No. 1.

Regarding composite isotropic shells we note, e.g. that the highest stress (compressive) in layer **c** of shell No. 23 (Table 6) is 49·5 per cent of the highest stresses (tensile and compressive) in shell No. 17.

(c) *Location of extremal stresses*

For the homogeneous shells Nos. 1–4, 17–18 the maximum tensile stresses occur in the ξ-direction at the *inner* fibers "4" whereas the highest compressive stresses in the ξ- and θ-directions appear at the *outer* fibers "1", all at the fixed edge $z = 0$.

Regarding composite orthotropic shells it is observed that maximum tensile stresses may occur at fibres "2" ($\zeta = 0$, $z = 0$), as in layer **b** of shell No. 8 (Tables 1, 3 and 5). Furthermore,

TABLE 3. ORTHOTROPIC LAYERS. CASE II

No.	Layers	τ_ξ (kg/cm^2)				τ_θ (kg/cm^2)				T_0 (°C)
	a	0	(2, 0)	−2064	(1, 0)	26	(2, 58)	−1439	(1, 0)	
1.										150
	a	2064	(4, 0)	0	(3, 5·6)	342	(4, 74)	−615	(3, 0)	
	â	0	(2, 4·9)	−1157	(1, 0)	27	(2, 42)	−1514	(1, 0)	
2										150
	â	1157	(4, 0)	0	(3, 0·5)	417	(4, 50)	−615	(3, 0)	
	b	133	(1, 42)	−7324	(1, 0)	49	(2, 86)	−2531	(1, 0)	
3										150
	b	7324	(4, 0)	−133	(4, 42)	569	(4, 102)	−1129	(3, 0)	
	b̂	0	(2, 0)	−1566	(1, 0)	68	(2, 30)	−3919	(1, 0)	
4										150
	b̂	1566	(4, 0)	0	(3, 0·2)	1193	(4, 34)	−1569	(3, 0)	
	a	—	—	−2828	(1, 0)	223	(2, 70)	−1668	(1, 0)	
5										112
	b	5386	(4, 0)	−1813	(3, 0)	1698	(4, 86)	−1101	(3, 0)	
	b	3471	(2, 0)	−6152	(1, 0)	—	—	−2367	(1, 0)	
6										187
	a	2624	(4, 0)	−490	(3, 26)	674	(4, 78)	−781	(3, 3·9)	
	â	—	—	−2077	(1, 0)	496	(2, 58)	−2066	(1, 0)	
7										112
	b	5423	(4, 0)	−2612	(3, 0)	6	(4, 14·5)	−1213	(3, 0)	
	b	4638	(2, 0)	−5549	(1, 0)	—	—	−2283	(1, 0)	
8										187
	â	1235	(4, 0)	−604	(3, 16·4)	1069	(4, 62)	−994	(3, 2·7)	
	a	751	(2, 0)	−1197	(1, 0)	—	—	−1179	(1, 0)	
9										112
	b̂	664	(4, 0)	−268	(4, 16·8)	681	(4, 38)	−1437	(3, 0·6)	
	b̂	—	—	−2383	(1, 0)	325	(2, 38)	−4872	(1, 0)	
10										187
	a	3094	(4, 0)	—	—	518	(4, 0)	−693	(3, 0)	
	â	233	(2, 5·2)	−984	(1, 0)	—	—	−1410	(1, 0)	
11										112
	b̂	830	(4, 0)	−67	(3, 0)	617	(4, 38)	−1255	(3, 0)	
	b̂	—	—	−1708	(1, 0)	132	(2, 34)	−4085	(1, 0)	
12										187
	â	1820	(4, 0)	—	—	682	(4, 0)	−651	(3, 0·8)	
	a	550	(2, 0)	−1499	(1, 0)	—	—	−1269	(1·0)	
13										150
	â	1049	(4, 0)	−202	(3, 15·1)	553	(4, 54)	−682	(3, 1·4)	
	â	—	—	−1629	(1, 0)	205	(2, 50)	−1798	(1, 0)	
14										150
	a	2114	(4, 0)	−73	(3, 0)	224	(4, 0)	−637	(3, 0)	
	b	4267	(2, 0)	−4324	(1, 0)	—	—	−2111	(1, 0)	
15										150
	b̂	744	(4, 0)	−897	(3, 10·6)	1693	(4, 42)	−2410	(3, 1·5)	
	b̂	—	—	−3163	(1, 0)	1066	(2, 46)	−5782	(1, 0)	
16										150
	b	7478	(4, 0)	−2782	(3, 0)	294	(4, 0)	−1519	(3, 0)	

TABLE 4. ISOTROPIC LAYERS. CASE II

No.	Layers	τ_ξ (kg/cm^2)				τ_η (kg/cm^2)				T_0 (°C)
	c	0	(2, 0)	−1564	(1, 0)	29	(2, 50)	−1379	(1, 0)	
17										150
	c	1564	(4, 0)	0	(3, 54)	345	(4, 58)	−682	(3, 0)	
	d	0	(2, 0·6)	−7856	(1, 0)	156	(2, 50)	−6002	(1, 0)	
18										150
	d	7856	(4, 0)	0	(3, 2·3)	1552	(4, 50)	−3676	(3, 0)	
	e	0	(2, 2·6)	−450	(1, 0)	7	(2, 50)	−450	(1, 0)	
19										150
	e	450	(4, 0)	0	(3, 0)	117	(4, 66)	−169	(3, 0)	
	c	86	(1, 22)	−2524	(1, 0)			−1667	(1, 0)	
20										183
	d	6815	(4, 0)	−3453	(3, 0)	1566	(4, 46)	−4977	(3, 0)	
	d	3620	(2, 0)	−6549	(1, 0)	1085	(2, 42)	−5819	(1, 0)	
21										117
	c	2298	(4, 0)	−145	(4, 20·9)	341	(4, 54)	−372	(3, 3)	
	c	28	(2, 0)	−1433	(1, 0)			−1513	(1, 0)	
22										133
	e	1008	(4, 0)			392	(4, 0)			
	e	217	(1, 26)	−426	(1, 0)	177	(2, 50)	−438	(1, 0)	
23										167
	c	837	(4, 0)	−553	(3, 0)	331	(4, 0)	−812	(3, 0)	
	d	4256	(2, 0)	−6520	(1, 0)	1066	(2, 42)	−5815	(1, 0)	
24										109
	e	1638	(4, 0)			707	(4, 0)			
	e	415	(1, 22)	−1309	(1, 0)	257	(1, 26)	−879	(1, 0)	
25										191
	d	6149	(4, 0)	−4521	(3, 0)	1203	(4, 46)	−5312	(3, 0)	

the highest tensile stresses appear at fibers "3" ($\zeta = 0$), as in layer $\hat{\mathbf{b}}$ of shell No. 15 (Tables 1 and 5) at a distance z of about $\frac{1}{10}$ of the shell radius. Shell No. 9 (Table 5) is noted as the maximum tensile stress in its layer **a** occurs at the *outer* fibers "1". Similar observations hold for the compressive stresses, as well as for two-layer isotropic shells.

(d) *Comparison of thermal cases I, II and III*

It is noted that for the thermal fields denoted as "case I" and "case II" the constant inner temperature T_i is equal to the inner temperature of case III, at $\xi = \infty$ and $\xi = 0$, respectively.

Consequently, the comparison of the results for case III with those of cases I and II may have some bearing on the thermo-elastic edge effect of the semi-infinite composite shells under consideration.

For the homogeneous shells Nos. 1–4 and 17–19, it is seen that the stresses for case I approach from below the results for case III. The stress level in case II is also lower than the one of case III, but there are differences between the results for these two thermal fields. In particular we note that for shell No. 18 the tensile axial stress in Table 6 does not exist in Table 4.

TABLE 5. ORTHOTROPIC LAYERS. CASE III

No.	Layers	τ_ξ (kg/cm^2)				τ_θ (kg/cm^2)				T_0 (°C)
	a	461	(1, 30)	−2250	(1, 0)	90	(1, 46)	−1495	(1, 0)	
1										150
	a	2250	(4, 0)	−461	(4, 30)	265	(4, 0)	−798	(3, 2·7)	
	â	230	(1, 20·9)	−1145	(1, 0)	90	(1, 34)	−1507	(1, 0)	
2										150
	â	1145	(4, 0)	−230	(4, 20·9)	277	(4, 0)	−788	(3, 2·3)	
	b	1710	(1, 42)	−8297	(1, 0)	157	(1, 66)	−2668	(1, 0)	
3										150
	b	8297	(4, 0)	−1710	(4, 42)	409	(4, 0)	−1479	(3, 3·1)	
	b̂	284	(1, 15)	−1455	(1, 0)	211	(1, 22)	−3789	(1, 0)	
4										150
	b̂	1455	(4, 0)	−284	(4, 15)	651	(4, 0)	−1976	(3, 1·9)	
	a	265	(1, 38)	−3732	(1, 0)	260	(1, 58)	−1940	(1, 0)	
5										112
	b	7646	(4, 0)	−2943	(3, 0)	317	(4, 0)	−1773	(3, 2·3)	
	b	3684	(2, 0·9)	−6143	(1, 0·1)	7	(1, 54)	−2366	(1, 0·1)	
6										187
	a	2618	(4, 0)	−930	(4, 34)	376	(4, 0)	−807	(3, 4)	
	â	—	—	−2635	(1, 0)	589	(1, 50)	−2401	(1, 0)	
7										112
	b	7762	(4, 0)	−4231	(3, 0)	334	(4, 0)	−1854	(3, 1·9)	
	b	4859	(2, 0·8)	−5518	(1, 0·3)	—	—	−2278	(1, 0·3)	
8										187
	â	1220	(4, 0)	−831	(4, 26)	619	(3, 54)	−1025	(3, 2·9)	
	a	1010	(1, 17·6)	−1216	(1, 0)	—	—	−1185	(1, 0)	
9										112
	b̂	680	(4, 0)	−906	(4, 17·2)	613	(3, 34)	−2645	(3, 2·6)	
	b̂	—	—	−2240	(1, 0)	506	(1, 34)	−4704	(1, 0)	
10										187
	a	2908	(4, 0)	—	—	462	(4, 0)	−685	(3, 0)	
	â	453	(1, 16·1)	−1044	(1, 0)	—	—	−1446	(1, 0)	
11										112
	b̂	896	(4, 0)	−478	(4, 16·2)	383	(3, 30)	−2283	(3, 2·3)	
	b̂	55	(1, 17)	−1489	(1, 0)	376	(1, 30)	−3829	(1, 0)	
12										187
	â	1621	(4, 0)	−33	(4, 17·1)	562	(4, 0)	−654	(3, 0)	
	a	642	(1, 26)	−1506	(1, 0)	—	—	−1272	(1, 0)	
13										150
	â	1054	(4, 0)	−517	(4, 22)	265	(3, 46)	−899	(3, 2·8)	
	â	32	(1, 26)	−1749	(1, 0)	272	(1, 42)	−1869	(1, 0)	
14										150
	a	2284	(4, 0)	−141	(4, 26)	275	(4, 0)	−782	(3, 2)	
	b	4857	(2, 1·1)	−4427	(1, 0·4)	—	—	−2126	(1, 0·4)	
15										150
	b̂	744	(4·0)	−1440	(4, 18·4)	1244	(3, 38)	−3154	(3, 2·7)	
	b̂	—	—	−3420	(1, 0)	1047	(1, 42)	−6082	(1, 0)	
16										150
	b	8412	(4, 0)	−3387	(3, 0)	425	(4, 0)	−1724	(3, 1·1)	

TABLE 6. ISOTROPIC LAYERS. CASE III

No.	Layers	τ_ξ (kg/cm^2)				τ_θ (kg/cm^2)				T_c (°C)
	c	341	(1, 26)	−1683	(1, 0)	74	(1, 42)	−1415	(1, 0)	
17										150
	c	1683	(4, 0)	−341	(4, 26)	50	(4, 0)	−879	(3, 2·4)	
	d	1756	(1, 26)	−8711	(1, 0)	274	(1, 46)	−6122	(1, 0)	
18										150
	d	8711	(4, 0)	−1756	(4, 26)	209	(3, 50)	−4732	(3, 2·4)	
	e	93	(1, 26)	−460	(1, 0)	31	(1, 38)	−455	(1, 0)	
19										150
	e	460	(4, 0)	−93	(4, 26)	118	(4, 0)	−218	(3, 2·5)	
	c	535	(1, 22)	−2816	(1, 0)	100	(1, 34)	−1755	(1, 0)	
20										183
	d	7544	(4, 0)	−3818	(3, 0)	199	(3, 42)	−5183	(3, 1·1)	
	d	3941	(2, 0)	−7190	(1, 0)	297	(1, 42)	−5909	(1, 0)	
21										117
	c	2554	(4, 0)	−622	(4, 20·9)	311	(4, 0)	−775	(3, 3·8)	
	c	45	(2, 0)	−1552	(1, 0)	...	...	−1596	(1, 0)	
22										133
	e	1100	(4, 0)			437	(4, 0)	−7	(3, 3·1)	
	e	477	(1, 26)	−352	(1, 0·2)	360	(1, 38)	−401	(1, 0·2)	
23										167
	c	737	(4, 0)	−539	(3, 0)	261	(4, 0)	−834	(3, 1·4)	
	d	4814	(2, 0)	−7400	(1, 0)	...	...	−5938	(1, 0)	
24										109
	e	1880	(4, 0)	−43	(4, 19·7)	828	(4, 0)	...	...	
	e	710	(1, 22)	−1492	(1, 0)	498	(1, 26)	−971	(1, 0)	
25										191
	d	6815	(4, 0)	−4952	(3, 0)	...	...	−5396	(3, 0·5)	

Regarding the composite shells considered it is found that the results for case III can be approximated for many examples by the stress field obtained for case I, however for other examples case II is more suitable.

It is observed that for some shells the layer inversion effect may vary numerically when evaluated for the various thermal fields. The same observation also holds for the location of extremal stresses and efficiency of shell composition.

(e) *Distribution of radial displacement, resultants, moments and stresses*

The detailed variation of the radial displacement, resultants and couples along shell generator is shown in Figs. 3 and 4 for shells Nos. 2, 3, 7 and 8 when subject to the thermal field III. The extremal stresses for these shells are given in Table 5, from which it is clear that for shell No. 8 the lowest stresses are achieved, except for the compressive stresses of its layer **b**. (See Fig. 5).

The layer inversion effect and the efficiency of lamination is clearly exemplified by shell No. 8. Figures 3 and 4 show that the results for resultants and moments for the various

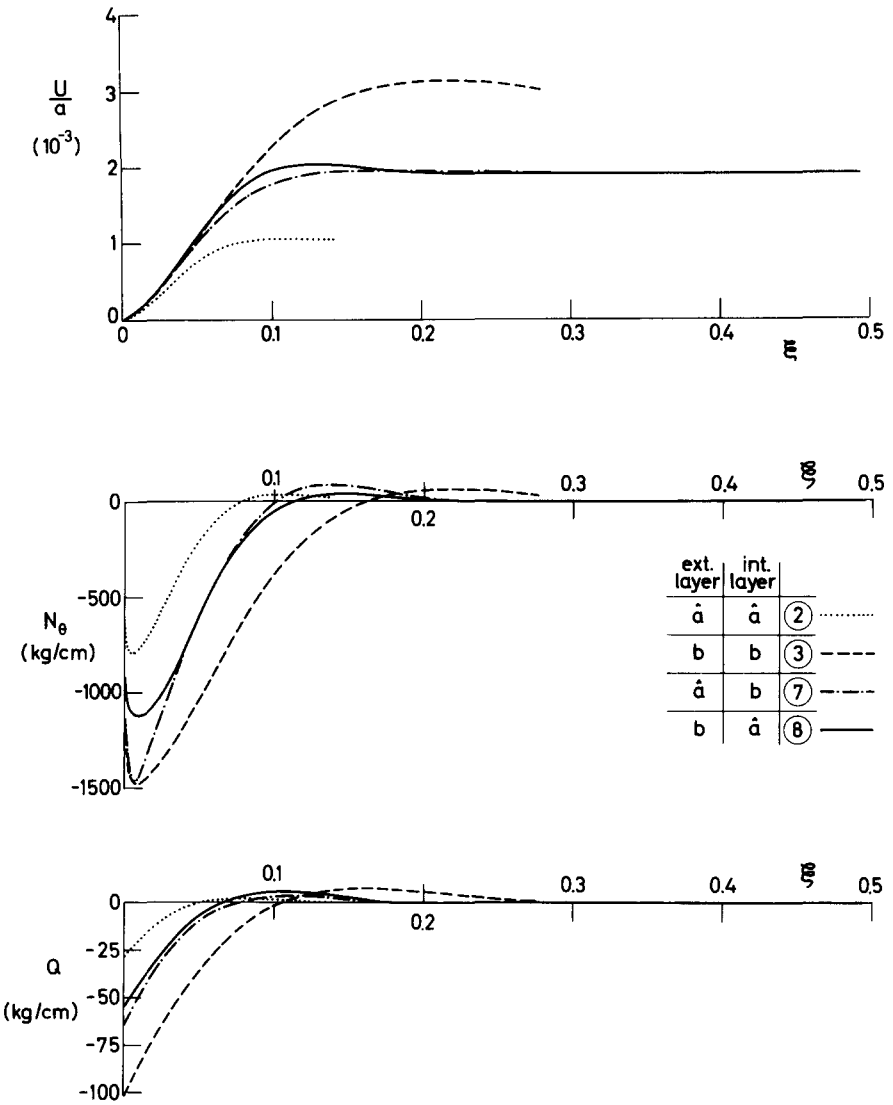

FIG. 3. Variation of radial displacement and stress resultants along shell generator.

shells are considerably different, quantitatively and qualitatively. It is noted that whereas for homogeneous shells, there is a relatively simple relationship for stresses in terms of resultants and couples—for heterogeneous shells the *cross-thermoelasticity effect*, shown by Stavsky [16], has to be considered. Consequently, it is quite impossible to foresee the detailed stress distribution just by observing Figs. 3 and 4. E.g. the compressive axial stress in layer **b** of shell No. 8 is *higher* by 31 per cent than the corresponding stress in shell No. 7 although M_ξ for the latter shell is over twice its value for shell No. 8, at $z = 0$. The thickness variation of the stresses at extremal locations are shown in Fig. 5 for shells No. 2, 3, 7 and 8.

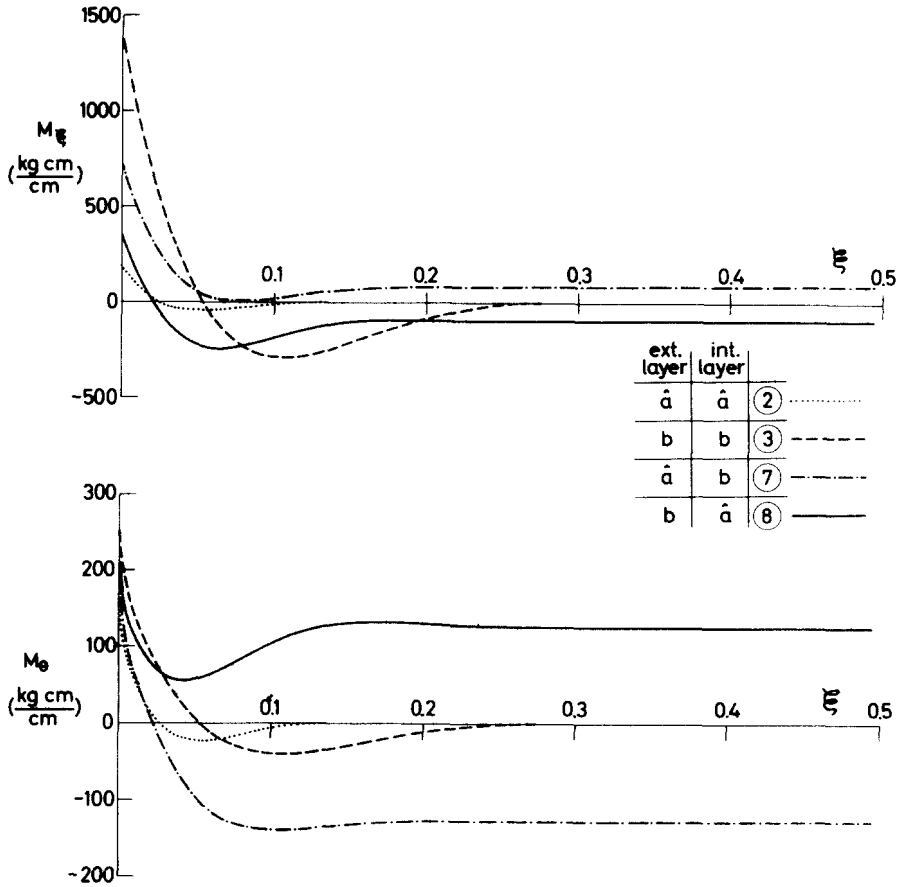

FIG. 4. Variation of axial and circumferential moments along shell generator.

6. CONCLUSIONS

The obtained results are remarkable for the following characteristics:

(1) The layer reversal effect was shown to *considerably* affect the stress field developed and its level. For a certain shell the stress went down to about *one tenth* of the corresponding stress for the very same composite shell when the order of the layers was reversed.

(2) The combined action of the layers composing the considered cylindrical shells was shown to provide, in many cases, a lower stress field than obtained for the individual constituents when acting as homogeneous shells.

(3) In view of Stavsky's [16] cross-thermoelasticity effect no clear indication of the detailed stress distribution can be obtained by observing the results for stress resultants and moments. Recurrence must be made to full coupled relations for stress components in terms of resultants and couples, as given by equation (28) of Ref. [16].

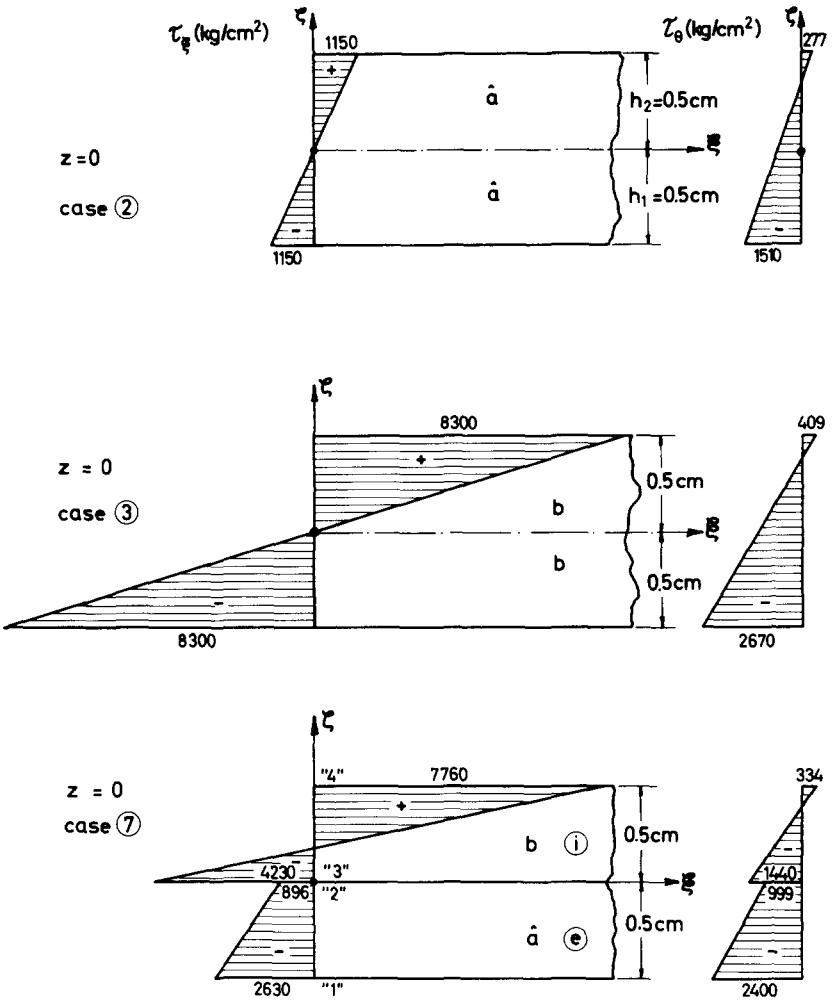

FIG. 5(a). Stress distribution at critical locations.

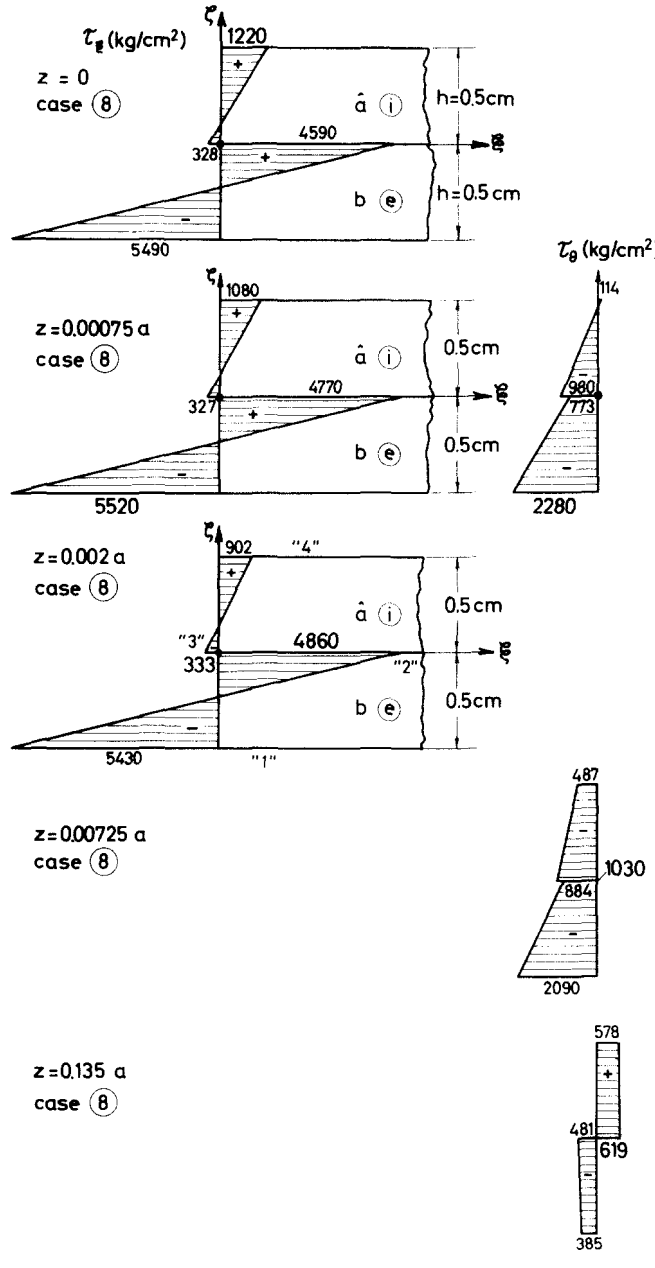

FIG. 5(b). Stress distribution at critical locations.

Acknowledgements—Preparation of this paper was supported by the Gerard Swope Foundation and by the Technion Research Funds.

The numerical examples were carried out at the Technion's Computation Center, helpfully discussed with S. Friedland.

REFERENCES

[1] J. M. C. DUHAMEL, *Mémoires par divers savants* **5**, 440 (1838). [Paper read before the Academy of Sciences on February 23, 1835].
[2] J. M. C. DUHAMEL, *Ecole Polytechnique* **15**, 1 (1837).
[3] F. NEUMANN, *Abhandlungen der deutschen Akademie der Wissenschaften* **2**, 1 (1841).
[4] E. MELAN and H. PARKUS, *Wärmespannungen infolge stationärer Temperaturfelder*. Springer (1953).
[5] H. PARKUS, *Thermoelasticity*. Blaisdell (1968).
[6] B. A. BOLEY and J. H. WEINER, *Theory of Thermal Stresses*. Wiley (1960).
[7] W. NOWACKI, *Thermoelasticity*. Pergamon Press (1962).
[8] H. PARKUS, *Sb. Öst. Akad. Wiss. Math. Nat. Kl. Abt. IIa* **160**, 1 (1951).
[9] Y. STAVSKY, *Contributions to Mechanics*, p. 181. M. Reiner 80th Anniversary Volume, edited by D. ABIR. Pergamon Press (1969).
[10] Y. STAVSKY, *Aeronaut. Q.* **15**, 29 (1964).
[11] Y. STAVSKY, *Proc. Fifth Int. Symp. Space Technology and Science*, p. 543. Tokyo (1964).
[12] A. C. ERINGEN, *Mechanics of Continua*, Chapter 8. Wiley (1967).
[13] Y. STAVSKY and N. J. HOFF, Mechanics of composite structures. Chapter 1 in *Composite Engineering Laminates*, edited by A. G. H. DIETZ. MIT Press (1969).
[14] Y. STAVSKY and S. FRIEDLAND, *Int. J. mech. Sci.* **11**, 217 (1969).
[15] H. S. CARSLAW and J. C. JAEGER, *Conduction of Heat in Solids*, 2nd edition, p. 42. Oxford University Press (1959).
[16] Y. STAVSKY, *AIAA Jnl.* **1**, 960 (1963).

(*Received* 21 *April* 1969; *revised* 9 *July* 1969)

Абстракт—Решаются осесимметрические линейные квази-статические термоупогие уравнения для составных ортотропных цилиндрических оболочек в замкнутом виде, для граничных условий защемленного типа.

Определяется случай полубесконечной оболочки в конечном виде. Исследуются разные комбинации слоистых оболочек. Оказывается, что 1/ неоднородность оболочек, или эффект замены слоя, в случае двухслойных оболочек, может значительно повлиять на полученное поле напряжений или его уровень; 2/ смешанное действие сложенных слоев превышает сумму индивидуальных свойств, и вызывает, в большинстве слчаев, новую характеристику, недостижимую составляющими в случае когда они работают как однородные оболочки; 3/ поперечно-упругий эффект вызывается распределением напряжений для рассматриваемых составных оболочек.